Electronic Supplementary Material (ESI) for RSC Advances.

Supporting information

Substitution reactivity and structural variability induced by tryptamine on the biomimetic rhenium tricarbonyl complex.

Frederick J. F. Jacobs[a] *Gertruida J. S. Venter,*[a] *Eleanor Fourie,*[a] *R. E. Kroon*[b] *and Alice Brink*[a*]

[a.] *Department of Chemistry, University of the Free State, PO Box 339, Bloemfontein 9300, South Africa.*
[b.] *Department of Physics, University of the Free State, Bloemfontein 9300, South Africa.*

* Corresponding author email: brinka@ufs.ac.za

SUPPLEMENTARY DATA FOR THE SUBSTITUTION OF METHANOL IN THE [Re(CO)$_3$(5Me-Sal-Tryptamine)(MeOH)] COMPLEX.

Table SI.1: (Figure 5) Temperature and [Py] dependence of the pseudo first-order rate constant for the formation of [Re(CO)$_3$(5Me-Sal-Tryptamine)(Py)] in methanol (λ = 380nm) with [Re(CO)$_3$(5Me-Sal-Tryptamine)(MeOH)] = 4 x 10^{-4} M.

[Py] (M)	k_{obs} at 5°C (s^{-1})	k_{obs} at 15.4°C (s^{-1})	k_{obs} at 25.3°C (s^{-1})
0.009	0.00221 ± 0.00002	0.0080 ± 0.0001	0.0241 ± 0.0001
0.024	0.00337 ± 0.00003	0.0169 ± 0.0002	0.0510 ± 0.0004
0.033	0.00396 ± 0.00004	0.0231 ± 0.0002	0.0707 ± 0.0004
0.048	0.00638 ± 0.00009	0.0312 ± 0.0003	0.0975 ± 0.0007
0.072	0.0111 ± 0.0005	0.0486 ± 0.0005	0.148 ± 0.001
0.095	0.0145 ± 0.0006	0.062 ± 0.001	0.199 ± 0.002

Table SI.2: (Figure SI.1) Temperature and [Imi] dependence of the pseudo first-order rate constant for the formation of [Re(CO)$_3$(5Me-Sal-Tryptamine)(Imi)] in methanol (λ = 380nm) with [Re(CO)$_3$(5Me-Sal-Tryptamine)(MeOH)] = 4 x 10^{-4} M.

[Imi] (M)	k_{obs} at 5°C (s^{-1})	k_{obs} at 15.6°C (s^{-1})	k_{obs} at 25.2°C (s^{-1})
0.010	0.00184 ± 0.00002	0.0082 ± 0.0001	0.0312 ± 0.0003
0.025	0.0046 ± 0.0001	0.0202 ± 0.0003	0.0478 ± 0.0005
0.035	0.0063 ± 0.0002	0.0233 ± 0.0003	0.0672 ± 0.0009
0.050	0.0092 ± 0.0006	0.0334 ± 0.0005	0.088 ± 0.002
0.076	0.016 ± 0.004	0.0473 ± 0.0006	0.132 ± 0.005
0.100	-	0.067 ± 0.001	0.179 ± 0.002

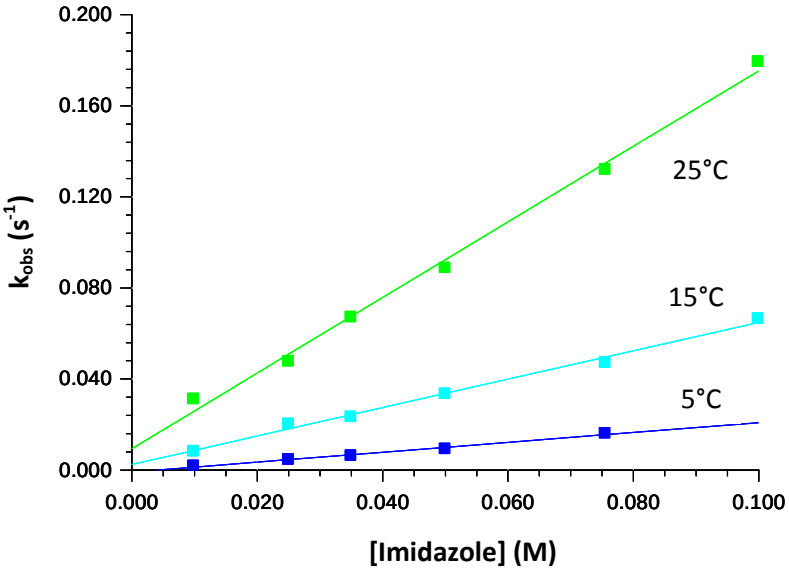

Figure SI.1: k_{obs} versus [imidazole] for the reaction of *fac*-[Re(CO)$_3$(5Me-Sal-Tryptamine)(MeOH)] and imidazole at different temperatures with [Re complex] = 4 x 10^{-4} M and [imidazole] = 0.01 M – 0.10 M collected at 380nm in methanol.

Table SI.3: Temperature and [DMAP] dependence of the pseudo first-order rate constant for the formation of [$Re(CO)_3$(5Me-Sal-Tryptamine)(DMAP)] in methanol (λ = 380nm) with [$Re(CO)_3$(5Me-Sal-Tryptamine)(MeOH)] = 4 x 10^{-4} M. (Using linear kinetic calculations)

[DMAP] (M)	k_{obs} at 6.1°C (s^{-1})	k_{obs} at 15.0°C (s^{-1})	k_{obs} at 25.0°C (s^{-1})
0.010	0.00634 ± 0.00009	0.0183 ± 0.0003	0.0311 ± 0.0003
0.025	0.0154 ± 0.0002	0.0393 ± 0.0005	0.0710 ± 0.0008
0.033	0.0158 ± 0.0002	0.0530 ± 0.0007	0.0924 ± 0.0009
0.050	0.0315 ± 0.0004	0.0700 ± 0.001	0.152 ± 0.001
0.075	-	-	0.225 ± 0.003
0.100	-	-	0.316 ± 0.003

Table SI.4: (Figure 6) Temperature and [DMAP] dependence of the pseudo first-order rate constant for the formation of [$Re(CO)_3$(5Me-Sal-Tryptamine)(DMAP)] in methanol (λ = 380nm) with [$Re(CO)_3$(5Me-Sal-Tryptamine)(MeOH)] = 4 x 10^{-4} M. (Using limiting kinetic calculations over a 2 order of magnitude concentration range.)

[DMAP] (M)	k_{obs} at 5.0°C (s^{-1})	k_{obs} at 15.1°C (s^{-1})	k_{obs} at 25.0°C (s^{-1})
0.010	0.0074 ± 0.0001	0.0102 ± 0.0001	0.0311 ± 0.0003
0.025	0.0162 ± 0.0001	0.0255 ± 0.0002	0.0710 ± 0.0008
0.035	0.0217 ± 0.0002	0.0373 ± 0.0003	0.0924 ± 0.0009
0.050	0.0308 ± 0.0002	0.0486 ± 0.0004	0.152 ± 0.001
0.075	0.0434 ± 0.0004	0.0724 ± 0.0006	0.225 ± 0.003
0.100	0.0518 ± 0.0006	0.0910 ± 0.0009	0.316 ± 0.003
0.250	0.107 ± 0.002	0.173 ± 0.002	0.542 ± 0.006
0.399	-	-	0.69 ± 0.01
0.400	0.136 ± 0.003	0.231 ± 0.002	-
0.500	0.164 ± 0.003	0.248 ± 0.003	-
0.762	-	-	0.85 ± 0.06

Table SI.5: (Figure SI.2) Temperature and [PPh_3] dependence of the pseudo first-order rate constant for the formation of [$Re(CO)_3$(5Me-Sal-Tryptamine)(PPh_3)] in methanol (λ = 380nm) with [$Re(CO)_3$(5Me-Sal-Tryptamine)(MeOH)] = 4 x 10^{-4} M.

[PPh_3] (M)	k_{obs} at 5°C (s^{-1})	k_{obs} at 15.4°C (s^{-1})	k_{obs} at 25.3°C (s^{-1})
0.002	0.001221 ± 0.000005	0.00824 ± 0.00007	0.0136 ± 0.0002
0.004	0.00131 ± 0.00001	0.01063 ± 0.00008	0.0154 ± 0.0002
0.008	0.00323 ± 0.00003	0.01490 ± 0.00005	0.0311 ± 0.0002
0.010	0.0049 ± 0.0001	0.0201 ± 0.0001	0.0422 ± 0.0002
0.025	0.0103 ± 0.0003	0.0462 ± 0.0003	0.1045 ± 0.0009
0.035	-	0.0699 ± 0.0006	0.159 ± 0.002

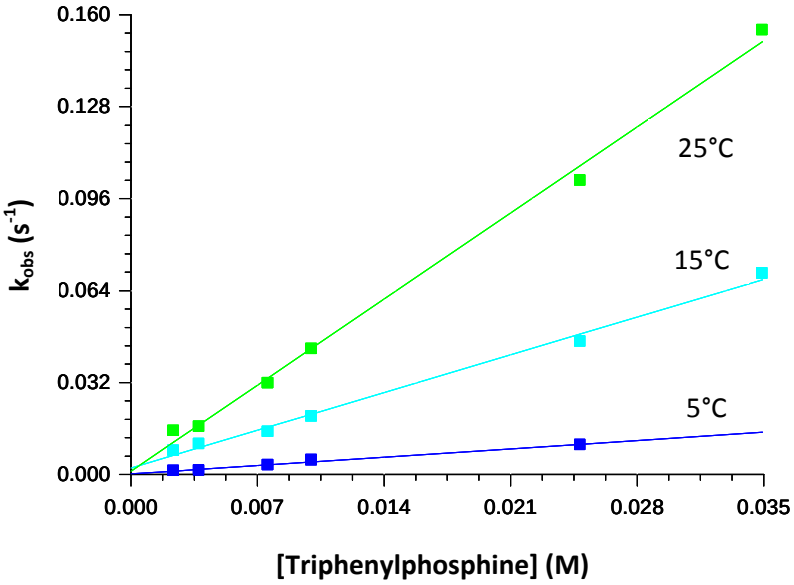

Figure SI.2: k_{obs} versus [Triphenylphosphine] for the reaction between *fac*-[Re(CO)$_3$(5Me-Sal-Tryptamine)(MeOH)] and triphenylphosphine at different temperatures with the [Re complex] = 4 x 10^{-4} M and [Triphenylphosphine] = 0.001 M – 0.035 M collected at 380nm in methanol.

Table SI.6: Eyring plots (from Equation 2) of the k_1 rate constants for the formation of [Re(CO)$_3$(5Me-Sal-Tryptamine)(L)] (where L = Py, Imi, DMAP and PPh_3) in methanol.

Pyridine	
1/T (x 10^{-3})	Ln(k_1/T)
3.597 ± 0.001	-7.868943 ± 0.000008
3.4674 ± 0.0001	-6.113573 ± 0.000006
3.3523 ± 0.0001	-4.98564 ± 0.00002

Imidazole	
1/T (x 10^{-3})	Ln(k_1/T)
3.597 ± 0.001	-7.156986 ± 0.000007
3.4650 ± 0.0001	-6.13561 ± 0.00001
3.3535 ± 0.0001	-5.19088 ± 0.00004

DMAP (Calculated from limiting traces)	
1/T (x 10^{-3})	Ln(k_1/T)
3.581 ± 0.001	-6.3 ± 0.6
3.4704 ± 0.0001	-5.6 ± 0.3
3.3540 ± 0.0001	-4.2 ± 0.1

DMAP (Calculated from linear traces)	
1/T (x 10^{-3})	Ln(k_1/T)
3.581 ± 0.001	-6.392 ± 0.001
3.4704 ± 0.0001	-5.83 ± 0.01
3.3540 ± 0.0001	-4.54 ± 0.02

Triphenylphosphine	
1/T (x 10^{-3})	Ln(k_1/T)
3.597 ± 0.001	-6.50720 ± 0.00001
3.4650 ± 0.0001	-5.03646 ± 0.00005
3.3546 ± 0.0001	-4.27860 ± 0.00009

Table SI.7: (Figure 9) Data for the plot of k_{obs} versus [Pyridine] (0.01 – 0.40 M) for *fac*-[Re(CO)$_3$(R-Sal-T)(MeOH)] (where R = H, CH_3 and T = *m*-toluidine, *p*-toluidine, phenylimine, 3-methylbutylimine, cyclohexylimine and tryptimine where λ = 440, 436, 441, 416, 417 and 380 nm respectively) complexes substituted with pyridine in methanol at 25°C.

Re-Salen-mTol			Re-Salen-3MeBu			Re-Salen-Cy	
[Py] (M)	k_{obs} (s^{-1})		[Py] (M)	k_{obs} (s^{-1})		[Py] (M)	k_{obs} (s^{-1})
0.050	0.076 ± 0.001		0.030	0.0473 ± 0.0009		0.025	0.077 ± 0.003
0.100	0.150 ± 0.002		0.041	0.081 ± 0.001		0.040	0.115 ± 0.003
0.200	0.282 ± 0.004		0.050	0.102 ± 0.001		0.050	0.147 ± 0.005
0.300	0.406 ± 0.007		0.200	0.370 ± 0.004		0.200	0.57 ± 0.01
0.400	0.54 ± 0.01		0.300	0.543 ± 0.007		0.300	0.82 ± 0.02
-	-		0.400	0.72 ± 0.01		0.400	0.99 ± 0.03

Re-Salen-Ph			Re-Salen-pTol			Re-SalH-Tryp	
[Py] (M)	k_{obs} (s^{-1})		[Py] (M)	k_{obs} (s^{-1})		[Py] (M)	k_{obs} (s^{-1})
0.025	0.0349 ± 0.0005		0.025	0.0394 ± 0.0006		0.009	0.0241 ± 0.0001
0.040	0.0576 ± 0.0009		0.040	0.0592 ± 0.0008		0.024	0.0510 ± 0.0004
0.050	0.072 ± 0.001		0.050	0.074 ± 0.001		0.033	0.0707 ± 0.0004
0.200	0.253 ± 0.006		0.200	0.281 ± 0.004		0.048	0.0975 ± 0.0007
0.300	0.393 ± 0.006		0.300	0.422 ± 0.005		0.072	0.148 ± 0.001
0.400	0.505 ± 0.009		0.400	0.562 ± 0.009		0.095	0.199 ± 0.002
-	-		-	-		0.397	0.82 ± 0.01

Table SI.8: (Figure SI.3) Data for the plot of k_{obs} versus [DMAP] (0.01 – 0.40 M) for *fac*-[Re(CO)$_3$(R-Sal-T)(MeOH)] (where R = H, CH$_3$ and T = *m*-toluidine, *p*-toluidine, phenylimine, 3-methylbutylimine, cyclohexylimine and tryptimine where λ = 440, 436, 441, 416, 417 and 380 nm respectively) complexes substituted with DMAP in methanol at 25°C.

Re-Salen-mTol			Re-Salen-3MeBu			Re-Salen-Cy	
[DMAP] (M)	k_{obs} (s^{-1})		[DMAP] (M)	k_{obs} (s^{-1})		[DMAP] (M)	k_{obs} (s^{-1})
0.043	0.089 ± 0.001		0.028	0.074 ± 0.001		0.026	0.097 ± 0.003
0.050	0.102 ± 0.001		0.042	0.11 ± 0.02		0.043	0.152 ± 0.003
0.102	0.193 ± 0.003		0.051	0.136 ± 0.002		0.054	0.199 ± 0.005
0.202	0.312 ± 0.005		0.206	0.458 ± 0.009		0.191	0.51 ± 0.01
0.290	0.402 ± 0.008		0.302	0.56 ± 0.02		0.308	0.75 ± 0.02
0.399	0.49 ± 0.01		0.418	0.66 ± 0.02		0.394	0.89 ± 0.03
0.568	0.59 ± 0.01		-	-		-	-
0.786	0.69 ± 0.01		-	-		-	-

Re-Salen-Ph			Re-Salen-pTol			Re-SalH-Tryp	
[DMAP] (M)	k_{obs} (s^{-1})		[DMAP] (M)	k_{obs} (s^{-1})		[DMAP] (M)	k_{obs} (s^{-1})
0.026	0.053 ± 0.001		0.026	0.0520 ± 0.0009		0.010	0.0311 ± 0.0003
0.043	0.077 ± 0.001		0.043	0.086 ± 0.001		0.025	0.0710 ± 0.0008
0.054	0.106 ± 0.002		0.054	0.108 ± 0.002		0.033	0.0924 ± 0.0009
0.191	0.286 ± 0.008		0.191	0.282 ± 0.006		0.050	0.152 ± 0.001
0.308	0.410 ± 0.009		0.308	0.387 ± 0.007		0.075	0.225 ± 0.003
0.394	0.45 ± 0.01		0.394	0.417 ± 0.009		0.100	0.316 ± 0.003
-	-		-	-		0.250	0.542 ± 0.006
-	-		-	-		0.399	0.70 ± 0.01
-	-		-	-		0.762	0.85 ± 0.06

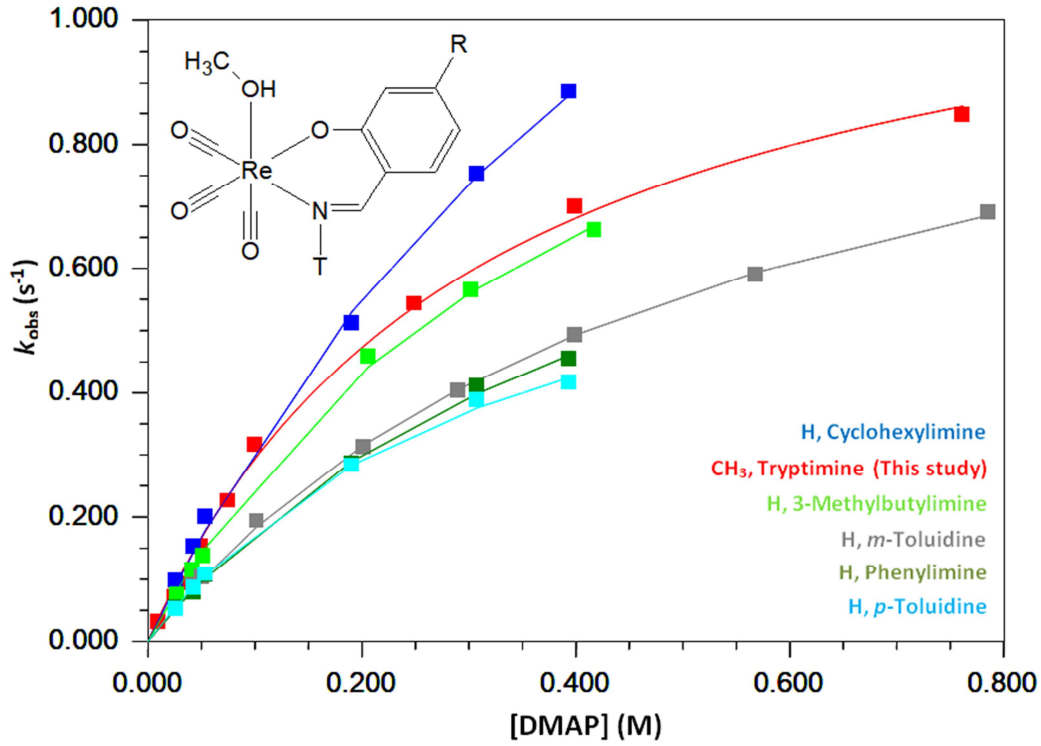

Figure SI.3: Plot of k_{obs} versus [DMAP] (0.01 – 0.40 M) for *fac*-[Re(CO)$_3$(R-Sal-T)(MeOH)] complexes (where R = H, CH$_3$ and T = *m*-toluidine, *p*-toluidine, phenylimine, 3-methylbutylimine, cyclohexylimine and tryptimine; λ = 440, 436, 441, 416, 417 and 380 nm respectively) substituted with DMAP in methanol at 25°C.

Below is an excerpt from the paper titled: *Solid State Isostructural Behavior and Quantified Limiting Substitution Kinetics in Schiff-Base Bidentate Ligand Complexes fac-[Re(O,N-Bid)(CO)$_3$(MeOH)]^n*.[1] Utilized in the calculations of linear versus limiting kinetics.

Monitoring the kinetics at conditions where [L] ≫ [Re], with typical metal concentrations ranging from 1×10^{-4} to 5×10^{-4} M, yields the rate equation for this scheme as defined in eq 2 for limiting kinetics (i.e. interchange mechanisms)

$$k_{obs} = \frac{k_3 K_2 [L]}{(1 + K_2[L]) + k_{-3}} \tag{2}$$

Here K_2 is the pre-equilibrium constant, k_3 the observed second-order limiting rate constant, and k_{-3} is the reverse reaction rate constant indicated by the graphical fits of k_{obs} versus ligand concentration.[2, 3] The substitution of methanol in the *fac*-[Re(L,L'-Bid)(CO)$_3$(MeOH)] complexes for a range of entering ligands can also be defined by the overall equilibrium

$$[Re(L, L' - Bid)(CO)_3(HOCH_3)] + L \underset{k_{-1}}{\overset{k_1 K_1}{\rightleftharpoons}} [Re(L, L' - Bid)(CO)_3(L)] + HOCH_3 \tag{3}$$

The pseudo-first-order rate constant was obtained from absorbance versus time data to determine the relationship for the profiles wherein linear dependences of k_{obs} versus [Ligand] were observed,

as described previously,[20,21] while the overall stability constant (K_1) has been determined kinetically using the definition

$$K_1 = \frac{k_1}{k_{-1}} \tag{4}$$

The linear concentration dependence of the pseudo-first-order rate constant (k_{obs}) assuming the overall equilibrium defined in eq 3 can be given determined from

$$k_{obs} = k_1[L] + k_{-1} \tag{5}$$

The overall rate equation (eq 5) will only be applicable at low ligand concentrations for the limiting mechanism before saturation limits have been reached, i.e., where linear second-order rate behavior occurs ($k_f = k_1 = k_3K_2$). The total forward rate constant (k_f) for an interchange mechanism will be similar to the overall second-order rate constant (k_1) within experimental error provided that data from well before the plateau is realized are used. However, at high ligand concentrations, limiting kinetics will dominate, and $k_f \neq k_1$.

End of excerpt. From the following reference: [1]A. Brink, H. G. Visser and A. Roodt, *J. Inorg. Chem.*, 2014, **53**, 12480–12488.

Table SI.9: UV-Vis kinetic data obtained from the k_{obs} vs ligand concentration plots for the substitution of methanol in *fac*-[Re(CO)$_3$(5Me-Sal-Tryptamine)(MeOH)] by different ligands (L) at different temperatures in methanol when calculated with limiting kinetics traces.

Entering ligands (L)	Tempera-ture (°C)	k_3 (s^{-1})	K_2 (M^{-1})	$k_f = k_3K_2$ ($M^{-1}s^{-1}$)
Py[1]	5.0	-0.05 ± 0.06	-3 ± 2	0.11 ± 0.18
	15.4	121 ± 18575	0.005 ± 0.81	0.6 ± 138
	25.3	-1.9 ± 0.5	-0.9 ± 0.2	1.8 ± 0.6
Imi[2]	5.0	-0.032 ± 0.007	-4.3 ± 0.6	0.14 ± 0.03
	15.6	-0.36 ± 0.39	-1 ± 1	0.5 ± 0.7
	25.2	-0.6 ± 0.2	-2.2 ± 0.5	1.3 ± 0.5
DMAP[3]	6.1	0.78 ± 0.27	0.67 ± 0.26	0.2 ± 0.2
	15.0	0.33 ± 0.04	3.24 ± 0.79	0.9 ± 0.2
	25.0	1.19 ± 0.03	3.79 ± 0.35	3.7 ± 0.3
PPh_3[4]	5.0	0.08 ± 0.06	6 ± 6	0.5 ± 0.6
	15.4	-0.15 ± 0.03	-9 ± 1	1.3 ± 0.3
	25.3	-0.5 ± 0.2	-7 ± 2	3 ± 1

[1] Concentration range of [Py] = 0.01–0.10 M [2] [Imi] = 0.01–0.10 M [3] [DMAP] = 0.01–0.10 M [4] [PPh_3] = 0.0025–0.0350 M.

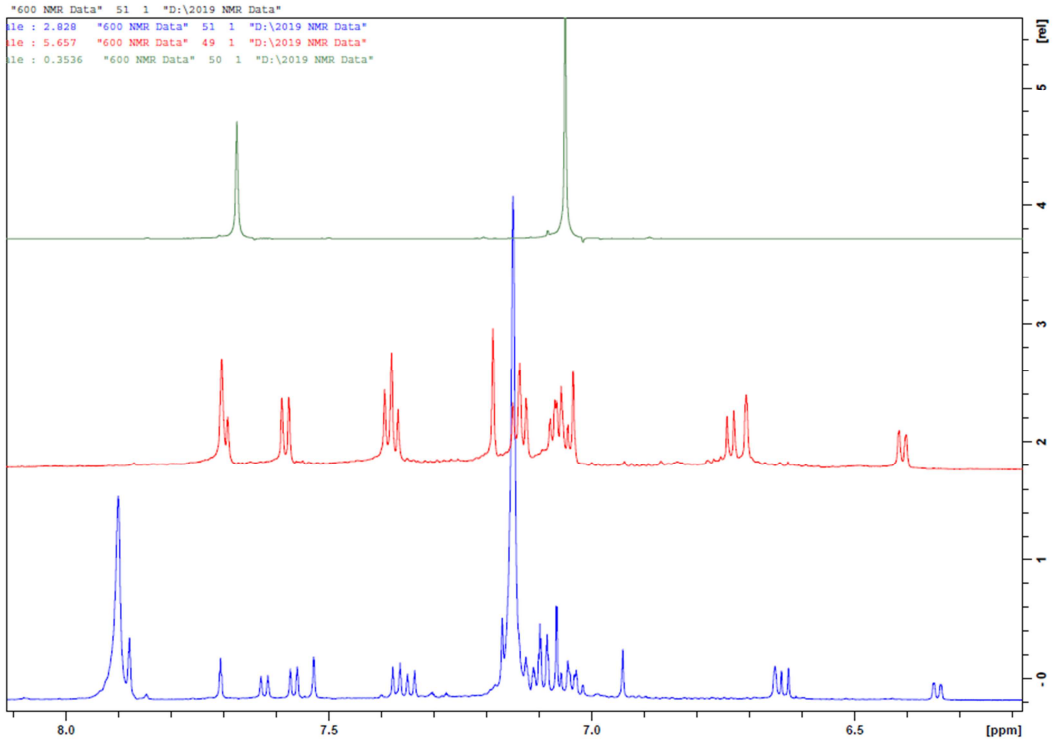

Figure SI.4: Aromatic region for the ^{1}H spectra of imidazole (green), *fac*-[Re(CO)$_3$(5Me-SalH-Tryp)(MeOH)] (red) and *fac*-[Re(CO)$_3$(5Me-SalH-Tryp)(Imidazole)] (blue) all in deuterated methanol. 2 equivalents excess of imidazole was added to the deuterated methanol-metal solution.

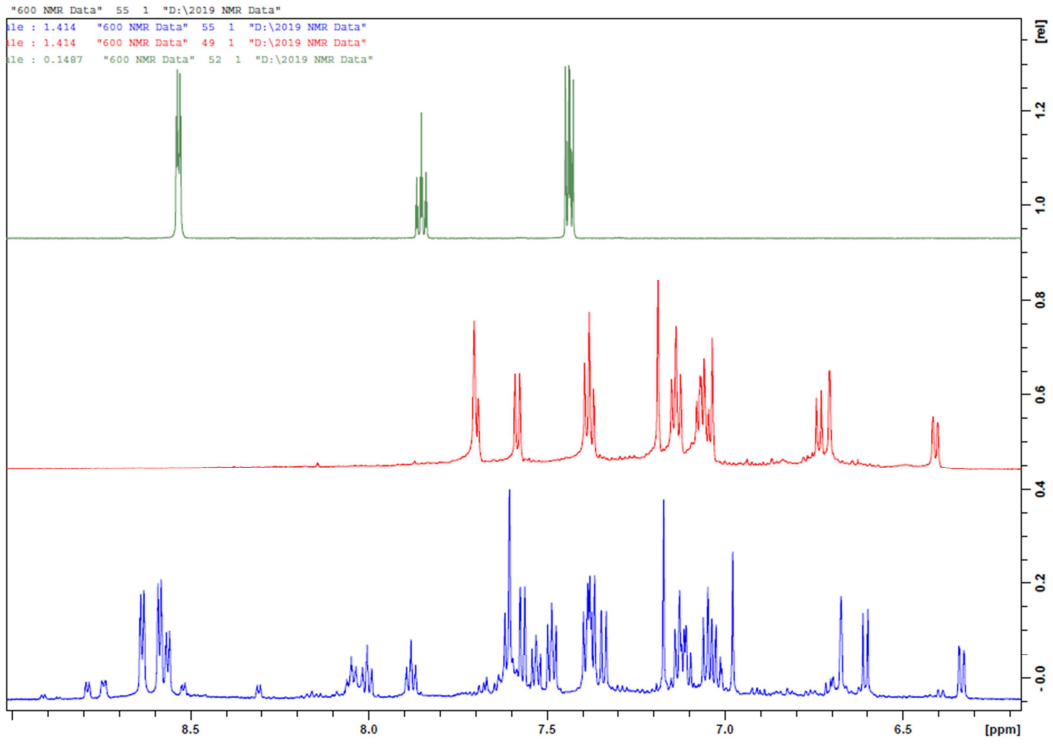

Figure SI.5: Aromatic region for the ^{1}H spectra of pyridine (green), *fac*-[Re(CO)$_3$(5Me-SalH-Tryp)(MeOH)] (red) and *fac*-[Re(CO)$_3$(5Me-SalH-Tryp)(Pyridine)] (blue) all in deuterated methanol. 2 equivalents excess of pyridine was added to the deuterated methanol-metal solution.

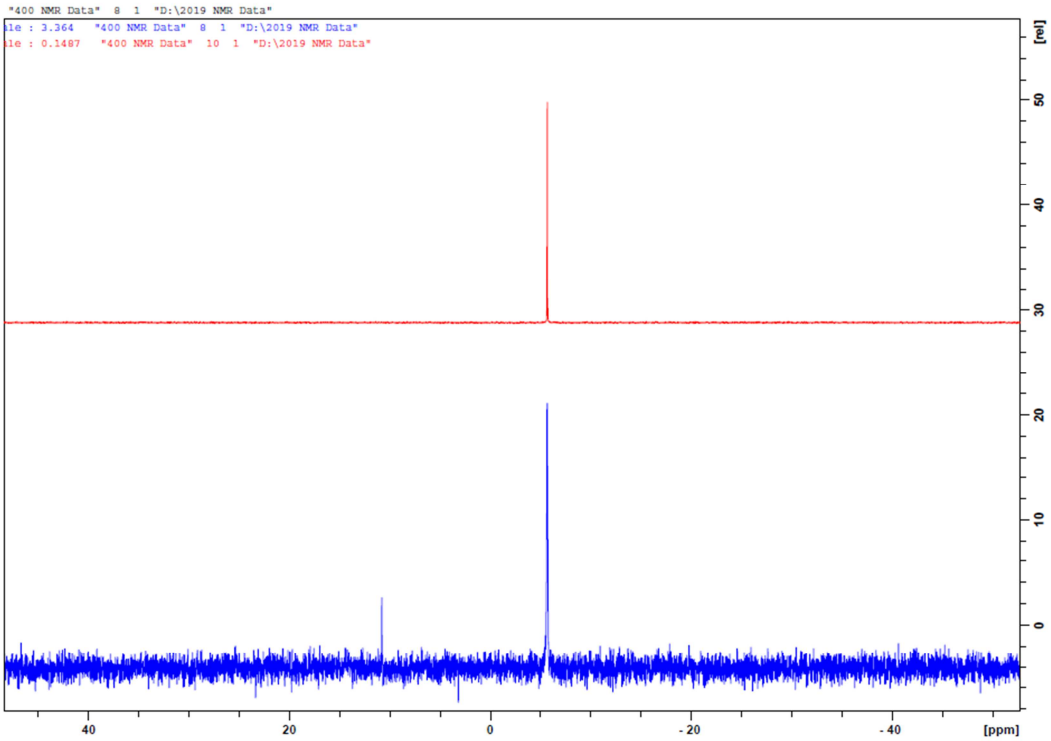

Figure SI.6: Full ^{31}P spectra of triphenylphosphine (red) and *fac*-[Re(CO)$_3$(5Me-SalH-Tryp)(PPh$_3$)] (blue) both in deuterated chloroform (PPh$_3$ has difficulty dissolving in methanol). 2 equivalents excess of PPh$_3$ was added to the deuterated chloroform-metal solution.

CELL TESTING:

Table SI. 9: The IC50 values (the concentration needed, in µM, to inhibit 50% of the growth of cancer cells) of each of the seven compounds versus Cisplatin along with the standard error.

Compound	IC50	Std err	IC50	Std err	IC50	Std err	Average	Std err
Cisplatin	**3.163**	1.4	**2.898**	1.6	**2.167**	2.1	**2.74**	3.0
5MeSalH-Tryptamine **(1)**	**14.90**	1.3	**25.95**	1.4	**1.791**	1.8	**14.2**	2.6
fac-[Re(CO)$_3$5MeSal-Tryp(MeOH)] **(2)**	**16.74**	1.3	**16.67**	1.5	**1.475**	1.6	**11.6**	2.5
fac-[Re(CO)$_3$5MeSal-Tryp(Py)] **(3)**	**21.76**	1.3	**28.37**	1.7	**12.01**	1.9	**20.7**	2.9
fac-[Re(CO)$_3$5MeSal-Tryp(Imi)] **(4)**	**15.42**	1.4	**8.166**	1.5	**18.36**	1.3	**14.0**	2.4
fac-[Re(CO)$_3$5MeSal-Tryp(PPh$_3$)] **(5)**	**26.35**	1.3	**9.124**	1.5	**30.41**	1.3	**22.0**	2.4
fac-[Re(CO)$_3$5MeSal-Tryp(DMAP)] **(6)**	**21.11**	1.5	**54.43**	1.6	**109.7**	1.3	**61.7**	2.5
fac-[Re(CO)$_3$5MeSal-Tryp]$_2$ **(7)**	**48.31**	1.7	**2.613**	1.5	**29.75**	1.3	**26.9**	2.6

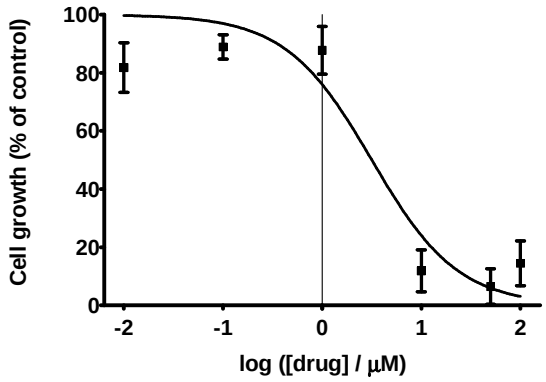

Figure CT.1: Graphical representation of the IC50 curve for Cisplatin.

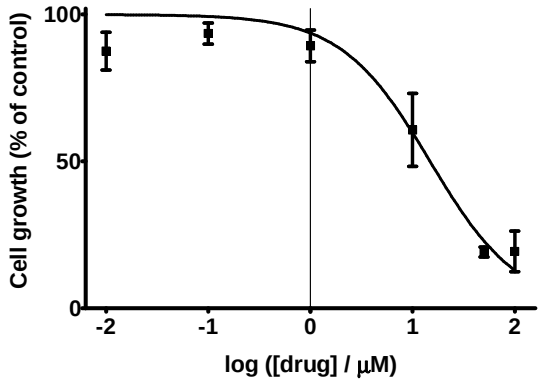

Figure CT.2: Graphical representation of the IC50 curve for 5MeSal-Tryptamine (1).

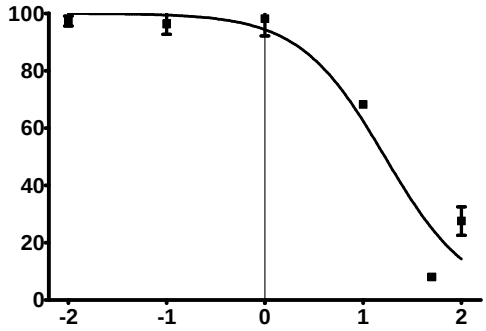

Figure CT.3: Graphical representation of the IC50 curve for *fac*-[Re(CO)$_3$5MeSal-Tryp(MeOH)] (2).

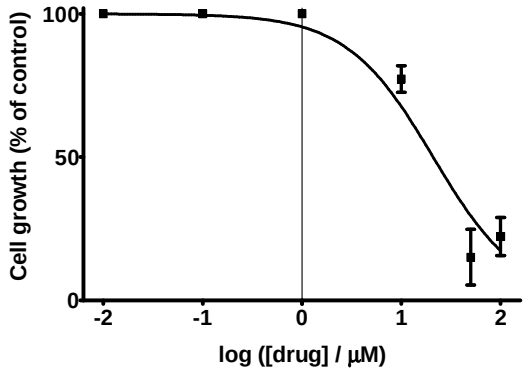

Figure CT.4: Graphical representation of the IC50 curve for *fac*-[Re(CO)$_3$5MeSal-Tryp(Py)] (3).

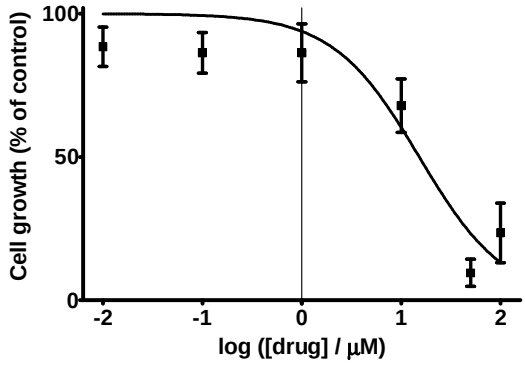

Figure CT.5: Graphical representation of the IC50 curve for *fac*-[Re(CO)$_3$5MeSal-Tryp(Imi)] (4).

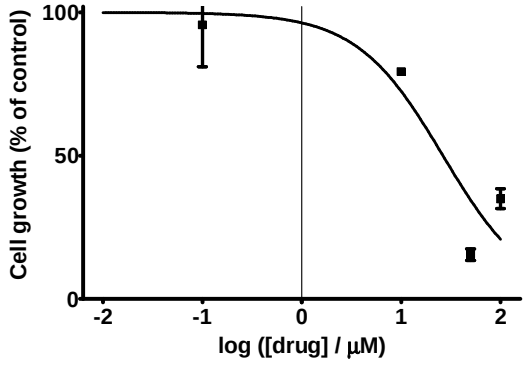

Figure CT.6: Graphical representation of the IC50 curve for *fac*-[Re(CO)$_3$5MeSal-Tryp(PPh$_3$)] (5).

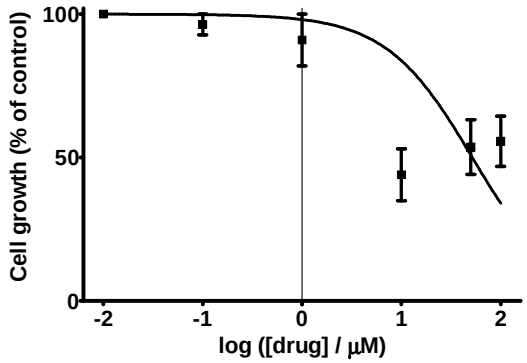

Figure CT.7: Graphical representation of the IC50 curve for *fac*-[Re(CO)$_3$5MeSal-Tryp(DMAP)] (6).

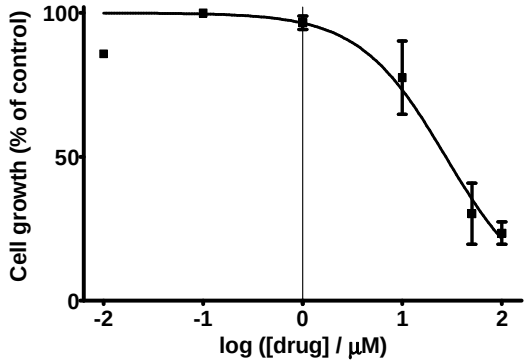

Figure CT.8: Graphical representation of the IC50 curve for *fac*-[Re(CO)$_3$5MeSal-Tryp]$_2$ (7).

PHOTOLUMINESCENCE:

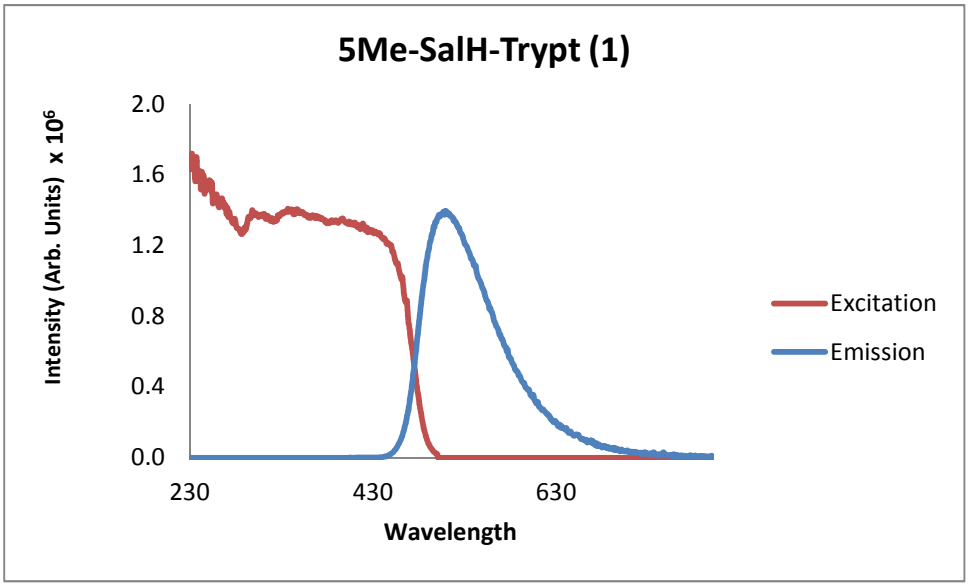

Figure PL.1: Excitation and emission graph of 5MeSalH-Tryptamine (1).

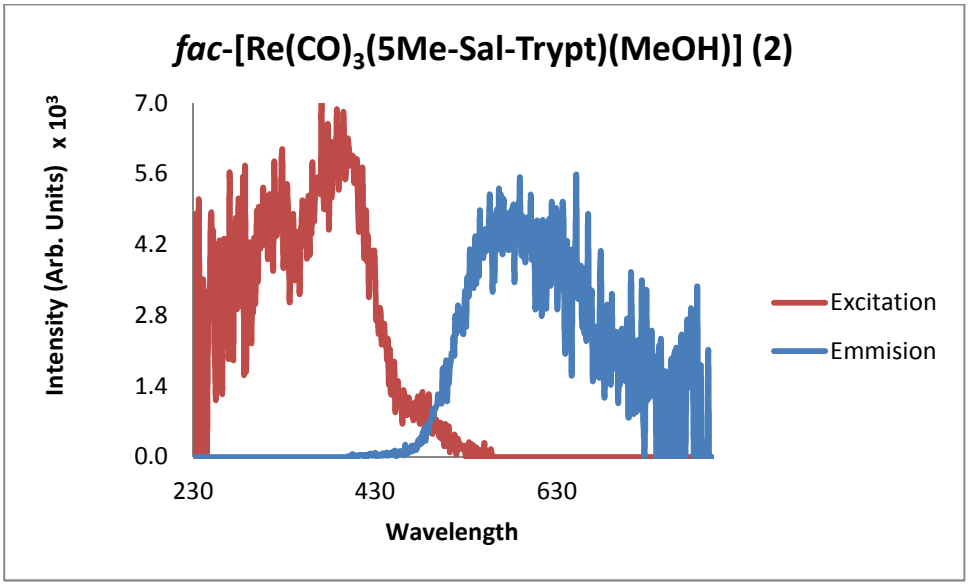

Figure PL.2: Excitation and emission graph of *fac*-[Re(CO)$_3$(5Me-Sal-Trypt)(MeOH)] (2).

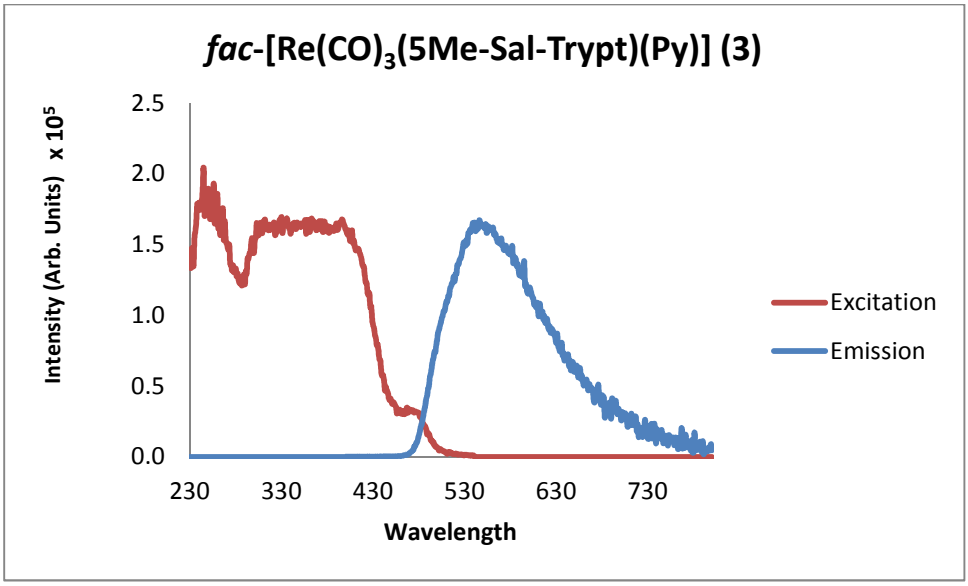

Figure PL.3: Excitation and emission graph of *fac*-[Re(CO)$_3$(5Me-Sal-Trypt)(Py)] (3).

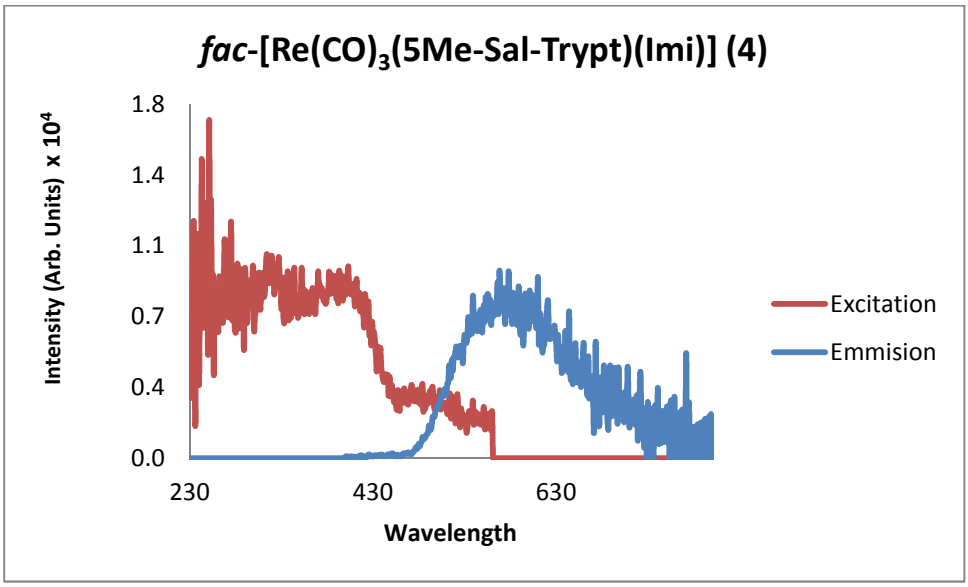

Figure PL.4: Excitation and emission graph of *fac*-[Re(CO)$_3$(5Me-Sal-Trypt)(Imi)] (4).

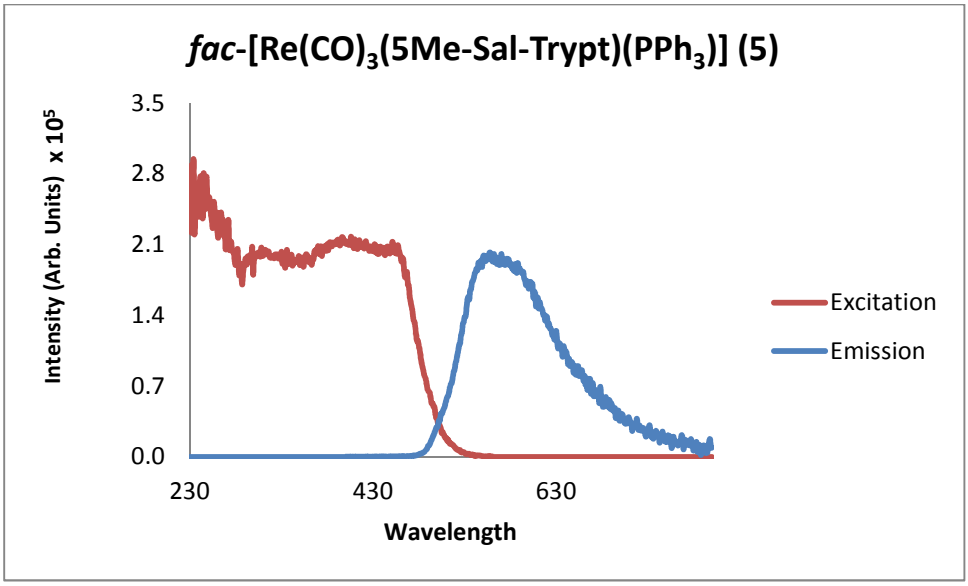

Figure PL.5: Excitation and emission graph of *fac*-[Re(CO)$_3$(5Me-Sal-Trypt)(PPh$_3$)] (5).

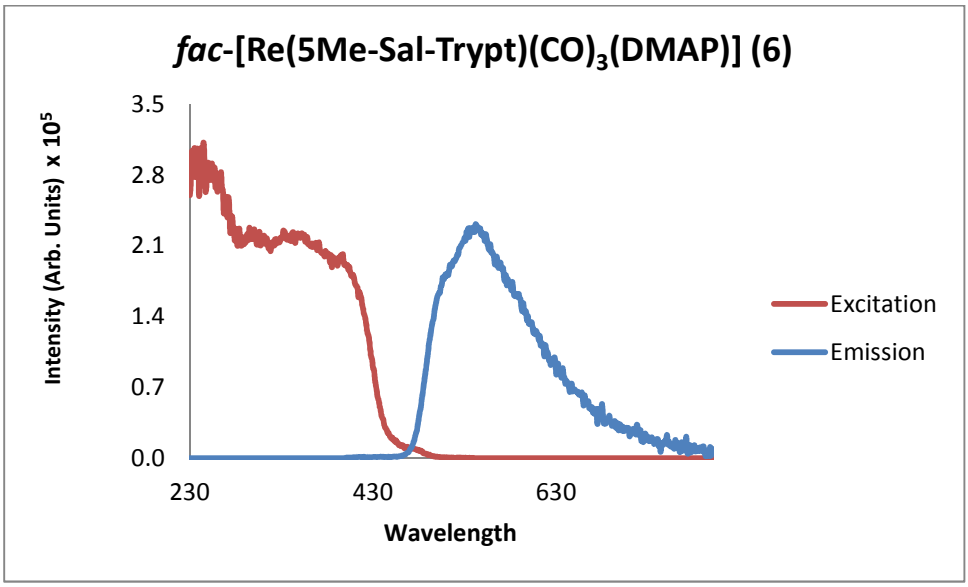

Figure PL.6: Excitation and emission graph of *fac*-[Re(CO)$_3$(5Me-Sal-Trypt)(DMAP)] (6).

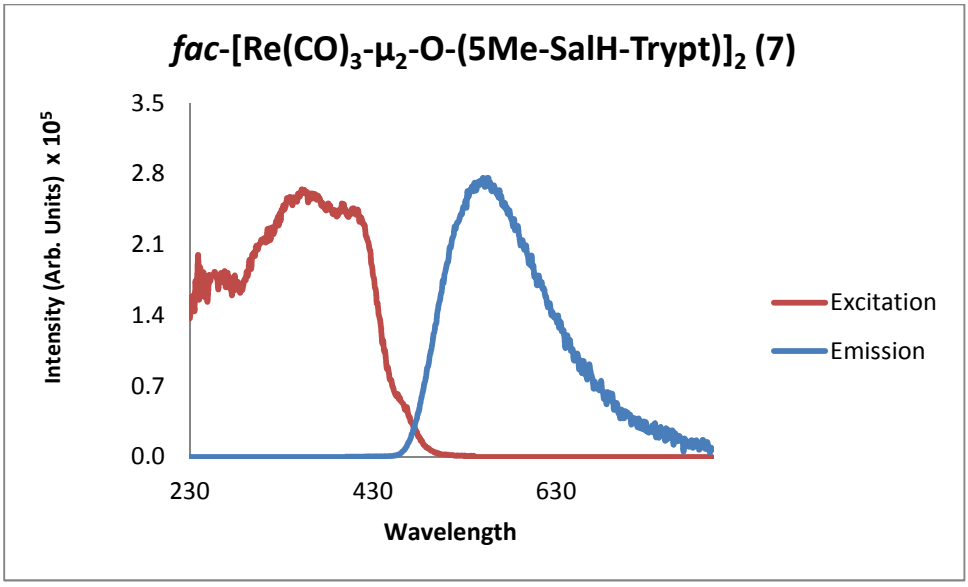

Figure PL.7: Excitation and emission graph of *fac*-[Re(CO)$_3$-μ$_2$-O-(5Me-SalH-Trypt)]$_2$ (7).

[1] A. Brink, H. G. Visser and A. Roodt, *J. Inorg. Chem.*, 2014, **53**, 12480–12488

[2] T.W. Swaddle, *Adv. Inorg. Bioinorg. Mech*. **1983**, *2*, 95-138.

[3] Wilkins, R.G. *Kinetics and Mechanism of Reactions of Transition Metal Complexes*, 2nd Ed., VCH Publishers, Inc., New York, USA, 2002